

## Experimental and numerical investigation of composite conical shells' stability subjected to dynamic loading

Sina Jalili<sup>\*1</sup>, Jamal Zamani<sup>1</sup>, M. Shariyat<sup>1</sup>, N. Jalili<sup>2</sup>, M.A.B. Ajdari<sup>1</sup> and M. Jafari<sup>1</sup>

<sup>1</sup>Mechanical Engineering Faculty, Khaje Nasir University of Technology, Tehran, Iran

<sup>2</sup>Mechanical Engineering Faculty, Amirkabir University of Technology, Tehran, Iran

(Received January 11, 2013, Revised December 19, 2013, Accepted January 11, 2014)

**Abstract.** In this article, stability of composite conical shells subjected to dynamic external pressure is investigated by numerical and experimental methods. In experimental tests, cross-ply glass woven fabrics were selected for manufacturing of specimens. Hand-layup method was employed for fabricating the glass-epoxy composite shells. A test-setup that includes pressure vessel and data acquisition system was designed. Also, numerical analyses are performed. In these analyses, effect of actual geometrical imperfections of experimental specimens on the numerical results is investigated. For introducing the imperfections to the numerical models, linear eigen-value buckling analyses were employed. The buckling modes are multiplied by very small numbers that are derived from measurement of actual specimens. Finally, results are compared together while a good agreement between results of imperfect numerical analyses and experimental tests is observed.

**Keywords:** composites shells; stability; pressure vessel; pressure rise time; critical pressure; imperfection; numerical method

### 1. Introduction

Shells have great extended applications in transportation industries, particularly in aerospace vehicles. In recent years employing of composite materials in manufacturing of shells has led to high strength to weight ratios. Stability analysis of thin walled shells that subjected to external loads is one of first design necessities. Generally aerospace vehicles such as ballistic missiles have supersonic velocities and continuous changing the density of surround medium can cause to apply suddenly dynamic loadings. In these sever conditions stability of shells can be in peril. Because of complex action of inertial forces during dynamic phenomenon, pure theoretical analysis can lead to under or over estimate designs. Hence, experimental tests have valuable place in these complicated design conditions.

Dynamic buckling of shells, in comparison with static stability analyses, is limited in literature. For example, Aksogan and Sofiyev (2002) investigated the dynamic buckling of isotropic cylindrical shells with variable thickness under external pressure, theoretically. Also same authors (2004), in other research studied dynamic stability of conical shells with variable thickness under

---

\*Corresponding author, Ph.D. Student, E-mail: [Sinajalily@hotmail.com](mailto:Sinajalily@hotmail.com)

lateral pressure. In other work, buckling of orthotropic conical shells with variable thickness under a time dependent external pressure has been studied by Sofiyev (2003). Eslami and Shariyat (1999) developed a high order numerical procedure based on finite difference formulation to explore dynamic buckling and postbuckling of laminated cylindrical shells. Fatt and Pothula (2010) investigated the stability of laminated cylindrical shells under impulsive loads using Mathieu stability criteria. Also they made a comparison between analytical results and ABAQUS commercial code simulations. Dumir *et al.* (2003) studied axisymmetric static and dynamic buckling of thick laminated conical shells by employing a high order finite element method. Effect of non-homogeneity on the stability of orthotropic conical shells has been considered in an article by Zerin (2012). Approach of this work is analytical and Galerkin method is implemented to reduce partial differential equations to a system of algebraic ones. Topal (2013) used FSDT theory to model a composite conical shell and by changing of fibers orientation optimized its stability and vibration characteristic. Elasto-plastic stability analyses has been investigated for predicting of buckling loads and postbuckling behavior of sandwich conical shells by Zielnica (2012).

There is a considerable shortage in the published experimental researches on the shells dynamic buckling. Humphreys *et al.* (1965) carried out some experiments on the shallow spherical shells under shock loading for finding the stability behavior of these shells. Dynamic axisymmetric snap-through response of elastic clamped shallow spherical shells was considered experimentally by Huang (1969). Tawadros *et al.* (1973) conducted some experiments for exploring the non-linear dynamic response of shells under blast waves. Dynamic pulse buckling of cylindrical shells under lateral pressures has been investigated by Anderson *et al.* (1968). Stiffened shells have extended use in industry because of considerable weight efficiency. Dynamic response of these types of structures also is discussed experimentally. Lakshmikantham (1974) studied the dynamic buckling of isotropic axially stiffened cylindrical shells under axial step loading. Dynamic axial plastic buckling of stringer stiffened cylindrical shells was investigated by Jones and Papageorgiou (1982).

In this paper has been tried to study buckling of composite truncated conical shells under combined axially and laterally dynamic loading by aid of both numerical and experimental methods. Numerical procedure has been based on two main steps and done in ABAQUS/Standard/Explicit environment. First, linear eigen-value analyses were performed on geometrically perfected shells to extract eigenvalue buckling loads and modeshapes. In next step, these mode shapes are used to building imperfections that will apply on perfect shells. Deviation of nodes' coordinates from perfect geometry is calculated based on linear buckling mode shapes multiplied by small numbers inspired from actual imperfection measurements. Also an experimental setup was designed and fabricated for making a comparison between results.

## 2. Experimental investigation

### 2.1 Manufacturing of specimens

There are several methods for manufacturing of composite materials. The characteristics of every method are different and must be considered in all aspects of a project. Hand lay-up procedure is a general way for making composite shells. Unlimited shape and dimension of shells are fabricated in this manner is one of advantages of this method. Also the simplicity and low cost of manufacturing in this way must be added to prominences. Furthermore some disadvantages are



Fig. 1 Fabricated wooden molds

Table 1 Nominal geometrical dimensions of wooden molds

Part name	$L$ (mm)	$R1$ (mm)	$R2$ (mm)
Small	110	55	110
Medium	170	55	137.5
Big	220	55	167.5

Table 2 Mechanical characteristics of resin and laminate

Material	Tensile Elasticity Module (GPa) $E_x=E_y$	In-plane Shear Modulus (GPa) $G_{xy}$	Poisson ratio $\nu_{xy}$	Yield Tensile stress (MPa)	Density ( $\text{kg/m}^3$ )
Woven fabric laminate	15	2.1	0.11	229	2010
Matrix (Epoxy resin)	4	1.5	0.38	130	1200

expectable in manufacturing of test specimens i.e., the quality of specimens are intensely depends on the worker or uncontrollable irregularities may be occurred.

For shaping the laminates to a conical shell, three wooden male molds are made. These molds are fabricated in three different geometries that variable in length of hypotenuse of truncated cone,  $L$  and constant vertex angle  $\gamma$  equal to  $30^\circ$  (Fig. 1). The nominal dimensions of molds are available in Table 1.

In this research, hand lay-up method was selected for fabricating of glass/epoxy composite conical shells. Reinforcements of matrix are plain-weave textiles with  $180 \text{ g/m}^2$  surface density that submerged in epoxy resin which cured in ambient temperature by aid of an amid-base hardener to make laminate. Hardener is mixed by resin in 1/10 mass ratio. Curing time is about 12-14 hours at  $25^\circ\text{C}$ . Mechanical characteristics of cured epoxy resin (Huntsman Co., Germany EEW-185) and laminate are offered in Table 2. Information in this table is obtained by ASTM 3039, 3518 and D 638, standard methods.

So specimens are made by the manner explained above by sticking the immersed stuffs in resin and turning around the molds. Also for obtaining various thicknesses of shells various number of stuff layers are employed. In this study the 2, 3 and 4 layers are considered. Fig. 2 shows the plain-weave ([0/90]) textiles that used in this investigation and final fabricated specimens.

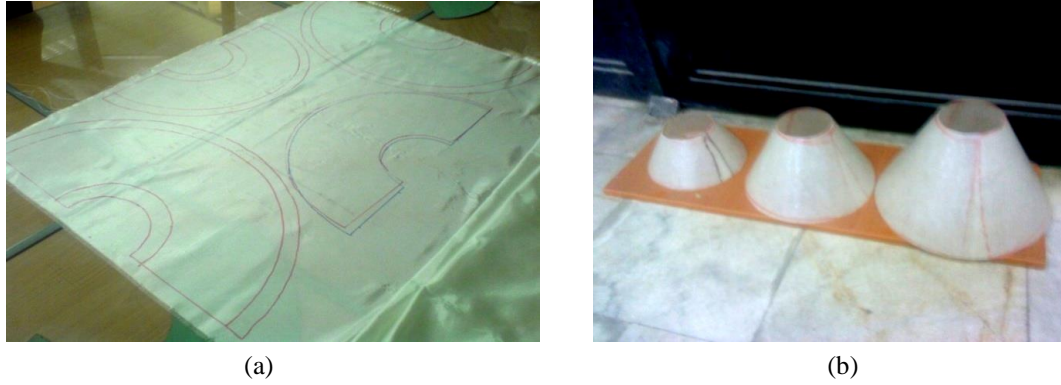


Fig. 2 (a) Woven fabrics and (b) specimens

What matter that has especial importance in this experimental study is deviation of dimensions of fabricated specimens with nominal ones that at initiation of design had been considered. For measuring the imperfections two geometrical aspects are mentioned: 1) variances in thickness of specimens and 2) horizontal sections deviation from perfect circle. Square of measured quantities variances is chosen for comparison

$$\zeta = \frac{\sqrt{(x_i - \bar{x})^2}}{n} \quad (1)$$

Where  $\zeta$ ,  $x_i$ ,  $\bar{x}$  and  $n$  are the imperfection scale, variables that can be radius or thickness, average quantity of variables and number of measured variables, respectively. Table 3 represents the actual geometrical dimensions of specimens. Measured variables are selected from random points on the specimens and oval form of sections is obtained by measuring the radius of specimens in multiple directions.

In this table also volume fraction of laminates is offered. For attaining this parameter a simple formula that based on the thickness of laminate is mentioned

$$v_f \% = \frac{t_f}{t_l} * 100 \quad (2)$$

Where  $v_f$  %,  $t_f$  and  $t_l$  are volume fraction percent, total employed textile layers thickness and laminate thickness, respectively. A single textile layer has 0.10 mm thickness.

For simplicity in recognizing the test specimens, simple codes that contain the first character of dimension of specimens and a number that refers to the layers that used in construction of them are employed, for example the code, S2 refers to the small specimen with 2 layers of stuff.

## 2.2 Setup for tests and data acquisition system

Because of low instability loads of manufactured specimens that are in range of atmospheric pressure, pneumatic method was chosen for applying pressure on shells. Pneumatic method has some advantages and also disadvantages i.e. test apparatuses are designed based on this procedure are relatively simple in comparison of hydraulics ones. Basically one of the simplicity sources of pneumatic systems comes back to this concept that there is no need to design any recirculation

Table 3 Actual geometrical dimensions of specimens

Specimen No.	$2R_1$ average (mm)	$2R_2$ average (mm)	$2h$ average (thickness) (mm)	$L$ (mm)	$\zeta$ (mm) thickness	$\zeta$ (mm) radius	$v_f\%$
S2	110.42	220.00	0.68	110.00	0.12	0.73	29.4
S3	110.42	220.00	0.98	110.00	0.16	0.85	30.6
S4	110.42	220.00	1.42	110.00	0.28	0.60	28.2
M2	110.56	275.74	0.68	167.02	0.17	0.87	29.4
M3	110.56	275.74	0.96	167.02	0.22	0.54	31.3
M4	110.56	275.74	1.42	167.02	0.23	0.64	28.2
B2	110.30	355.50	0.66	218.00	0.14	0.56	30.3
B3	110.30	355.50	0.98	218.00	0.13	0.34	30.6
B4	110.30	355.50	1.44	218.00	0.26	0.62	27.8

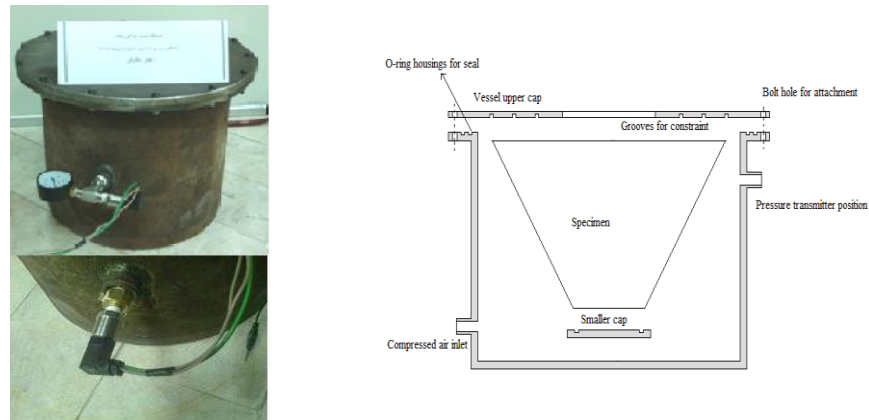


Fig. 3 Schematic and figure of pressure vessel

(Note: A dial pressure gauge was used for calibration of transmitter at start of the work)

parts to get back the used air to a reservoir. Also the risk level of pneumatic system are comparatively is low because of the application pressures range. Low costs of fabricating of pneumatic systems must be added to this list. In other hand some problems due to compressibility nature of air may be occurred. This phenomenon can cause to some non uniformities of pressure profile that act on structures or some inaccuracies in measuring of actual load. But with some considerations this difficulties can be reduced effectively.

One of approaches for decreasing the compressibility of air is to reduce the dead volume of pressure vessel. Also the sensor that measures the pressure acts on specimens is attached on a near position to them as possible as. For decreasing the dead volume, the vessel is designed near to the biggest test specimen's dimensions. Fig. 3 shows the of final designed pressure vessel. For constraining the specimens, three grooves with 4mm depth that were consistent with larger diameter of shells are used. These grooves are constructed on the upper cap of vessel. A polyethylene cap with a groove for closing the smaller end of shells is employed. For sticking the specimens on the grooves silicon seal glow was used. Also a hole in center of this cap is designed for visual considerations. The upper cap is attached to the vessel by 14, M8 ISO bolts and nuts.

For data acquisition part of system a pressure transmitter PT-2000 (DELTA Co., South Korea)



Fig. 4 The complete prepared setup of tests

with 0-4 bar application range is employed. Output signal of sensor was read by a 150 MHz oscilloscope. Also a computer, for storing the output graphs of oscilloscope is used. Fig. 4 illustrates the complete setup of test.

### 2.3 Tests performing and output signal interpretation

For dynamic pressurizing the test vessel, a 125 liters compressor was employed. By charging the compressor storage vessel to variable pressures and opening suddenly the connection valve between compressor storage and test vessels, achievement to the various loading rates was possible.

The pressure variation history was linear with a good approximation. After linear part of pressure increasing duration, because of large deformation of specimens during buckling, a tangible volume change was occurred in dead volume of test vessel and this phenomenon causes a disruption in pressure variation. Often this disruption illustrates itself by decreasing in pressure.

By considering the descriptions, mentioned above, two definitions are offered:

- *Pressure Rise Time*: refers to duration of linear part of pressure history and
- *Critical Dynamic Buckling load*: is the point that first disruption is detected.

Fig. 5 shows a typical pressure history and above definitions details on it.

Output voltage signals were converted to pressure by a linear relation that was depended on the shift of curves on the oscilloscope screen and sensor characteristics.

## 3. Numerical analyses

### 3.1 Imperfections and eigen value buckling analyses:

Numerical methods have extensive applications in engineering designs and scientific studies. However, robust results only can be gained by considering details about the all aspects of problem. For example, in real world, perfect structures are not achievable and generally, assumptions in theoretical studies are with simplifications. In studying stability of thin wall structures such as composite shells, effect of imperfections is more serious and must be in attention margin of designers. Investigation and recognizing of various sources of imperfection are challengeable

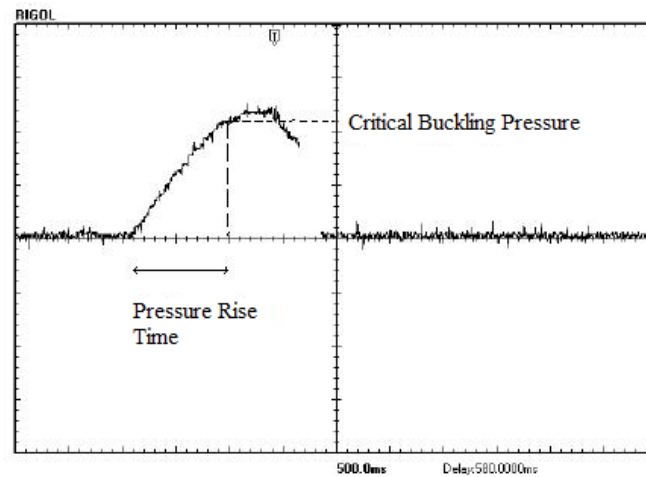


Fig. 5 Pressure history and definitions

fields of study in solid mechanics. Geometrical imperfections, material non-homogeneities and boundary conditions defects are renowned examples of structure related imperfections. Furthermore, some non predictable conditions that act on the distribution of loading can be one of other sources of deviation of analytical or numerical calculations from actual test results.

In this paper, geometrical imperfections including deviation of real shells from perfect circular sections and variation of thickness along circumference of shell are taken in account. Referring to the Table 3,  $\zeta$  in thicknesses and radiuses are utilized to building imperfections and applying to perfect structures with nominal dimensions.

But before everything, the procedure for configuration of geometrical imperfections must be selected. One of conventional methods is usage of eigenvalue linear buckling analyze as base of determination of buckling mode shapes. In next pace, these mode shapes are used as deviation shapes of imperfect structure from perfect one. The normalized mode shapes must be multiplied in very small numbers to change the locations of nodes in meshed model to simulate the real condition. Generally, a linear combination of a few first modes is utilized in building of ultimate shape of imperfect shell, and in this case first 10 modes of linear buckling analyses are selected. The small multiplied numbers in case of radius of circular sections; are inspired from values of deviation from average, ( $\zeta$  in radius) and in case of thicknesses the mentioned number ( $\zeta$  in thickness) is reduced from total average thickness of shells. For unifying the simulations, the averages of values of  $\zeta$  are calculated and used that in case of radius, value of 0.63 (mm) and in case of thickness, 0.19 (mm) are adopted.

In Fig. 6, exaggerated shapes of shells after introduction of imperfections are depicted.

### 3.2 Dynamic stability analysis

In next step, after introduction of imperfections to structures, dynamic stability numerical analysis must be performed. These analyses are affected from test results in a way that the PRTs that are obtained in experimental investigations used as base pressure rise times that studied in numerical surveys. In such a way, the target PRT and specimens are fixed and loading changes to



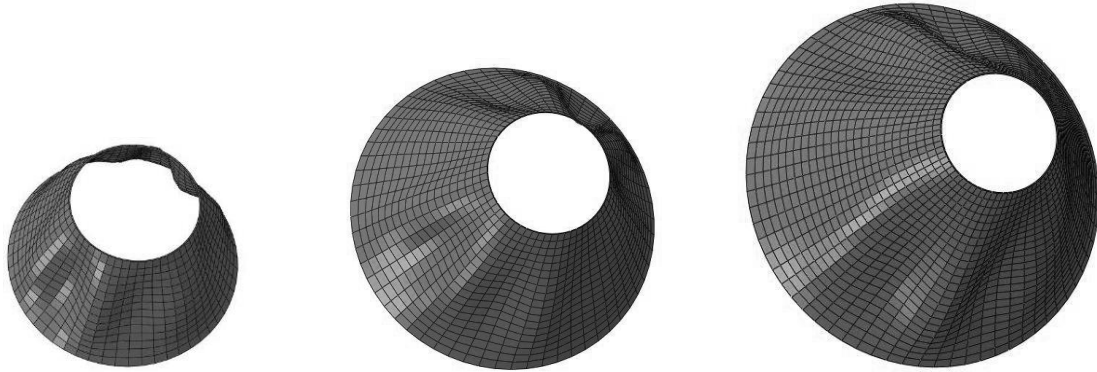


Fig. 6 Exaggerated shape of imperfect shells, (left to right: *S*, *M* and *B* specimens, magnification about 250 times more than what is real)

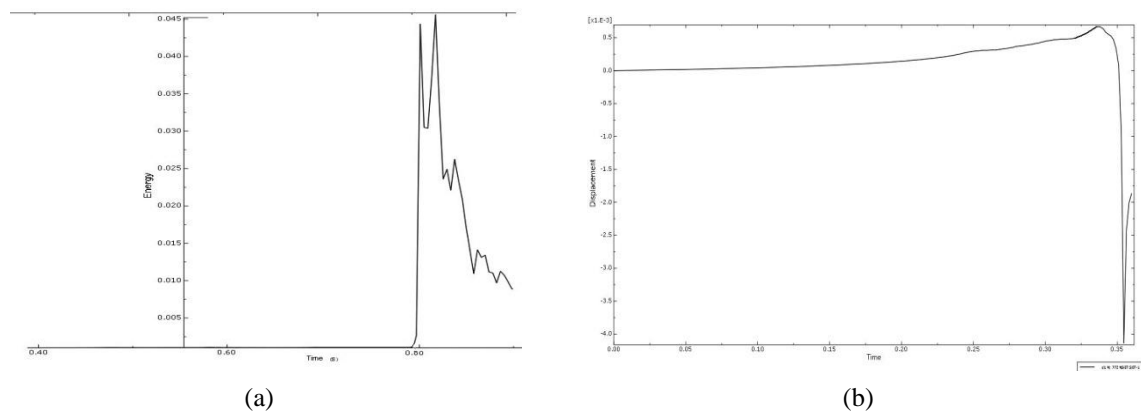


Fig. 7 Variation of (a) Kinetic energy of B4 in 0.8(s) PRT and (b) displacement of a node in middle circumference of M3 in 0.35 (s) PRT

instability conditions. So in a fixed time of loading, the maximum of linear pressure history that applied on shell gradually increased until achieving suddenly considerable change (snap-through phenomenon) in dynamic characteristics of structure such as kinetic energy or displacement in some selected nodes in middle circumference of shells. Very accurate coincidence between kinetic energy and displacement of nodes were observed in studies.

For example, variations in the history of above parameters in loading duration are illustrated in Fig. 7 for some specimens.

The maximum pressure of loading history cause to first instability signs of structures is recorded as dynamic pressure of stability.

#### 4. Results and discussion

This part of research accomplished by establishment of equivalence between woven fibers and



Table 4 Converted elastic coefficients of the woven fabric to a cross-ply laminate

$E_l=E_r$ (GPa)	$E_t=E_\theta$ (GPa)	$G_{lt}=G_{r\theta}$ (GPa)	$\nu_{lt}=\nu_{r\theta}$
26	4	2.1	0.4

multi-ply unidirectional laminates. Woven fibers are made of fibers oriented along two perpendicular directions. One is called the warp and the other is called weft direction. The fibers are woven together. For an approximation (with about 15%) of the elastic properties of the fabrics, it can be considered that stuff consisted of two plies of unidirectional at  $90^\circ$  angels with each other. By considering these notations:

$e$ = total layer thickness,

$n_1$ = number of warp yarns per meter,

$n_2$ = number of weft yarns per meter,

$$k = \frac{n_1}{n_1 + n_2},$$

Then, the equivalent thickness of each unidirectional fiber is:

$$e_{warp} = ke \quad (3)$$

$$e_{weft} = (1 - k)e \quad (4)$$

Because of type of the used woven fabric, magnitude of  $k$  will be equal to 0.5. So for finding the equivalent laminate mechanical properties it is enough to half the thickness of woven fabric and using below relations to evaluate new elastic constants (Gay *et al.* 2003)

$$E_l = \frac{1}{k} (E_x + (k - 1)E_t) \quad (5)$$

$$\nu_{lt} = \nu_{xy} \left( k + (1 - k) \frac{E_l}{E_t} \right) \quad (6)$$

Where,  $E_l$ ,  $E_t$  and  $\nu_{lt}$  are longitudinal elastic module, transverse elastic module and Poisson ratio of unidirectional lamina, respectively. In these equations,  $E_t$  is equaled to the matrix elasticity module. Feasibility of this assumption returns to the negligible load endurance of unidirectional fibers in transverse direction. Also there is no change in in-plane shear modulus of elasticity, that means

$$G_{xy} = G_{lt} \quad (7)$$

It's assumed that the shells were consisted of a cross ply ( $[0^\circ/90^\circ]$ ) laminate. Of course there are some deviations from this exact assumption that mainly returns to the technology of fabrication of specimens and turning the woven fabrics around the space curvature of molds.

After performing the numerical calculations and experimental tests, results were obtained. Tables 5-7 present the variation of dynamic buckling load of specimens versus pressure rise time (PRT). It is obvious that numerical results that relate to the eigenvalue analyses of perfect shells are considerably higher than experimental ones. There are some reasons for this phenomenon, for example imperfections have serious effects on the final results of experimental tests. Also the boundary conditions that are considered clamp here are not perfect and a little deviation may be occurred. Especially, these effects are bolded in buckling and stability tests.

Table 5 Stability analyses of small specimens ( $L/R1=2$ )

Spec. Code	$R1/2h$	Perfect Shell Eigen value Buckling Pressure(mbar)	PRT(s)	(Imperfect) Numerical Dynamic Buckling Pressure(mbar)	Experimental Dynamic Buckling Pressure(mbar)	Compressor Pre-charged Pressure (mbar)
S2	81.1	495	1.2	155	155	155
			0.8	175	175	175
			0.6	230	230	230
			0.4	265	265	265
S3	56.3	1451	1	350	340	510
			0.8	380	375	800
			0.6	445	450	1000
			0.4	485	475	1300
S4	38.6	2794	1.6	1210	1100	2500
			1.2	1300	1250	3000
			1	1340	1300	3500
			0.6	1400	1500	4000

Table 6 Stability analyses of medium specimens ( $L/R1=3$ )

Spec. Code	$R1/2h$	Perfect Shell First Eigen-value Buckling Pressure(mbar)	PRT(s)	(Imperfect) Numerical Dynamic Buckling Pressure(mbar)	Experimental Dynamic Buckling Pressure(mbar)	Compressor Pre-charged Pressure (mbar)
M2	81.1	230	0.4	130	120	400
			0.35	135	125	600
			0.3	145	130	1000
			0.25	150	130	2000
M3	56.4	811	0.7	195	190	440
			0.5	265	250	540
			0.4	285	275	800
			0.35	295	300	1200
M4	38.7	1577	1.5	575	550	1000
			1.1	600	565	1300
			0.9	685	625	1600
			0.7	710	625	2000

Another point is the dynamic buckling loads of specimens that have higher magnitudes than static ones. In better word, by decreasing the PRT, stability threshold of specimens enhances. This returns to the producing of more inertial forces that resist against the external pressure.

It is noteworthy here, that experimental magnitude of PRTs that are not same in all specimen cases, necessarily. Its reason comes back to the uncontrollable PRT parameter procedure of tests. Reaching to a special PRT parameter could not be possible by this method because this parameter depends on the specimen buckling load and compressor vessel charge pressure. Controlling both of these parameters may need more complex and also costly equipments.

Application of imperfection reduces the stability loads to near the feasible fringe of experimental tests. It can be inferred that geometrical imperfections have major share in

Table 7 Stability analyses of big specimens (L/R1=4)

Spec. Code	R1/2h	Perfect Shell First Eigen-value Buckling Pressure (mbar)	PRT(s)	(Imperfect) Numerical Dynamic Buckling Pressure (mbar)	Experimental Dynamic Buckling Pressure(mbar)	Compressor Pre-charged Pressure (mbar)
B2	81.2	142	1	35	Signal tracing was impossible for this specimen due to the low stability pressures.	
			0.9	40		
			0.6	65		
			0.3	85		
B3	56.3	511	0.5	185	190	600
			0.4	190	200	800
			0.25	215	220	1000
			0.2	260	275	1400
B4	38.6	984	1.8	380	330	500
			1.3	430	410	800
			1	550	520	1000
			0.8	615	610	1200

decreasing of stability threshold of shells. Introduction of imperfection to the shells lower the stability load from experimental results in some cases. In B3, M3, S3 and S4 this note can be observable. Calculations show that differences between imperfect numerical analyses and experimental ones are averagely less than seven percent. However deviations are confined in 14 percent and one percent range.

In bigger and also thinner shells effect of increasing rate of loading is more distinguishable. This is because of accelerating of shells' particles in easier manner that produce stronger inertial forces.

In Table 7, there is no experimental data for B2 specimen. Low level of stability pressures of this specimen cause to signal tracing became careless. Also available PRT data in this row are selected arbitrary only for comparison.

Exact tracing of buckling modes and counting lobes because of high happening rate of dynamic buckling phenomenon requires a high speed camera or dynamic strain gauges attached in multiple locations. But sometimes (such as S4 specimen case during conducting test at maximum available loading rate (PRT=0.6)), effects of produced buckling lobes remained on the specimen surface. Fig. 8 shows this specimen after test.

Of course this happening did not occur for other specimens. Thinner wall and more flexibility of those specimens cause to return to the rest condition after unloading without any remained effect. Also high ratio of flexibility to strength of used resin has important influence on high resilience of specimens.

Dimensionless numbers have special value in engineering and science. Here, by defining a dimensionless number  $\lambda$ , comparison between specimens can be more effective (Ross *et al.* 1999)

$$\lambda = \left( \frac{\sigma_p}{E_x} \right)^4 \sqrt[4]{\frac{\left( \frac{L}{2R_m \cos \gamma} \right)^2}{\left( \frac{2h}{2R_m \cos \gamma} \right)^3}} \quad (8)$$

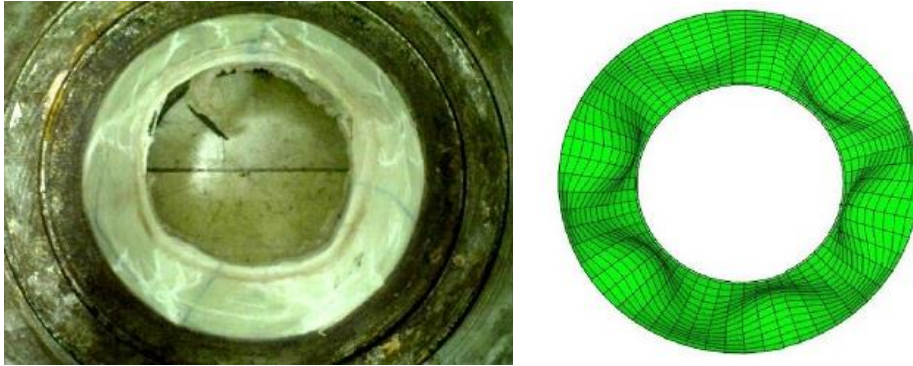


Fig. 8 Effects of buckling lobes on S4 specimen (Left), Result of numerical analysis (Right)

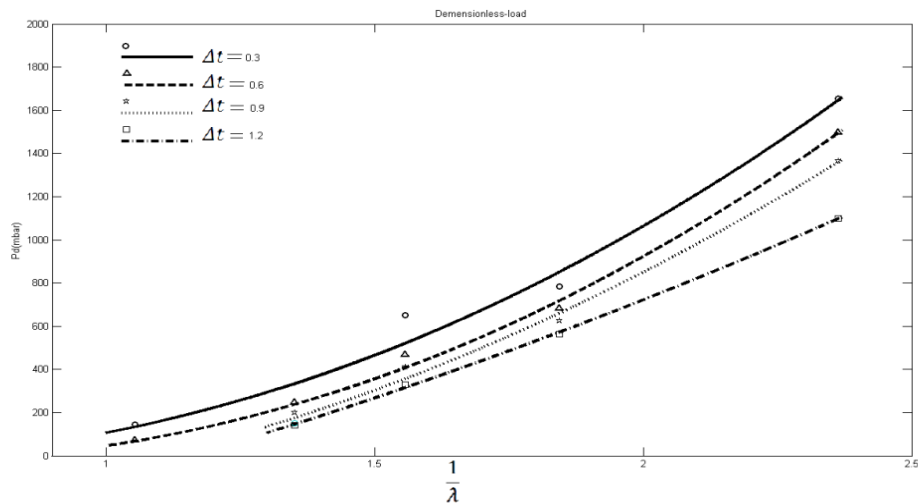


Fig. 9 Variation of experimental buckling pressures vs.  $1/\lambda$

Where  $R_m$  and  $\sigma_p$  refer to the average of minor and major radiuses of truncated cone and yield stress of material, respectively.

By using this number, comparing the specimens without need to group them is possible. Specimens with larger dimensions and thinner wall, have higher  $\lambda$  magnitude. Fig. 9 demonstrates variation of dynamic buckling pressure of specimens versus inverse of  $\lambda$ .

## 6. Conclusions

Dynamic stability analysis of composite truncated shells was carried out by numerical and experimental approaches. Buckling analyses have special sensitivity to the imperfections and so there is tremendous difference between perfect numerical and experimental results. Experimental tests that were conducted in this study show this fact transparently. Conclusions that were obtained in this research can be sorted as follow:

- In the pressure rise time ranges that tests were carried out, dynamic buckling pressure of manufactured specimens are higher than static magnitude ones. This returns to the complicated action of produced inertial forces that resist against applied pressure direction. By decreasing the PRT value this enhancement increases.
- Above result can lead to a valuable design point that by designing and testing specimens in static state, there will be a safety margin for dynamically loaded cases. This can reduce seriously costs and time consumptions.
- By paying attention to mentioned conclusions and developing more studies according to the special cases, more optimum design of sensitive and vital parts of high speed vehicles such as aerospace missiles or torpedoes can be possible.
- Imperfection studies show that by measuring geometrical imperfections and introduction them to numerical models of shells, results can be feasibly neared to experimental data. This is a valuable conclusion in design. Actual fringe stability threshold of shell structures under dynamic or static loads can be anticipated by low cost imperfection measurements and numerical analyses. At least these analyses are more reliable for structures having medium or low level of sensitivity to imperfections.

## References

- Aksogan, O. and Sofiyev, A.H. (2002), "Dynamic buckling of a cylindrical shell with variable thickness subject to a time-dependent external pressure varying as a power function of time", *J. Sound Vib.*, **254**(4), 693-702.
- Sofiyev, A.H. and Aksogan, O. (2004), "Buckling of a conical thin shell with variable thickness under a dynamic loading", *J. Sound Vib.*, **270**, 903-915.
- Sofiyev, A.H. (2003), "The buckling of an orthotropic composite truncated conical shell with continuously varying thickness subject to a time dependent external pressure", *Compos., Part B: Eng.*, **34**, 227-233.
- Eslami, M.R. and Shariyat, M. (1999), "A high-order theory for dynamic buckling and postbuckling analysis of laminated cylindrical shells", *J. Pres. Ves. Tech., ASME*, **121**, 94-102.
- Fatt, M.S.H. and Pothula, S.G. (2010), "Dynamic pulse buckling of composite shells subjected to external blast", *Compos. Struct.*, **92**, 1716-1727.
- Dumir, P.C., Dube, G.P. and Mulick, A. (2003), "Axisymmetric static dynamic buckling of laminated thick truncated conical cap", *Int. J. Nonlin. Mech.*, **37**, 903-910.
- Zerin, Z. (2012), "The effect of non-homogeneity on the stability of laminated orthotropic Conical shells subjected to hydrostatic pressure", *Struct. Eng. Mech.*, **43**(1), 89-103.
- Topal, U. (2013), "Pareto optimum design of laminated composite truncated circular Conical shells", *Steel Compos. Struct.*, **14**(4), 397-408.
- Zielnica, J. (2012), "Buckling and stability of elastic-plastic sandwich Conical shells", *Steel Compos. Struct.*, **13**(2), 157-169.
- Humphreys, R.S., Roth, R.S. and Zatlars, J. (1965), "Experiments on dynamic buckling of shallow spherical shells under shock loading", *AIAA J.*, **3**(1), 33-39.
- Haung, N.C. (1969), "Axisymmetric dynamic snap-through of elastic camped shallow spherical shells", *AIAA J.*, **7**(2), 215-220.
- Tawadros, K.Z. and Glockner, P.G. (1973), "Experiments on the non-linear dynamic response of shells under blast waves", *J. Sound Vib.*, **26**(4), 441-463.
- Anderson, D.L. and Lindberg, H.E. (1968), "Dynamic pulse buckling of cylindrical shells under transient lateral pressures", *AIAA J.*, **6**(4), 589-598.
- Lakshmikantham, C. and Tsui, T.U. (1974), "Dynamic stability of axially-stiffened imperfect cylindrical shells under axial step loading", *AIAA J.*, **12**(2), 163-169.

- Jones, N. and Papageorgiou, E.A. (1982), "Dynamic axial plastic buckling of stringer stiffened cylindrical shells", *Int. J. Mech. Sci.*, **24**, (1), 1-20.
- Gay, D., Hoa, S.V. and Tsai, S.W. (2003), *Composite Materials, Design and Applications*, CRC Press, New York, USA.
- Ross, C.T.F., Sawkins, D. and Johns, T. (1999), "Inelastic buckling of thick-walled circular conical shells under external hydrostatic pressure", *Ocean Eng.*, **26**, 1297-1310.